Phase calibration of sonar systems using standard targets and dual-frequency transmission pulses

Alan Islas-Cital, Philip R. Atkins,[a] and Kae Y. Foo
School of Electronic, Electrical and Computer Engineering, The University of Birmingham, Edgbaston, Birmingham, B15 2TT, United Kingdom

Ruben Picó
Instituto de Investigación para la Gestión Integrada de Zonas Costeras, Universitat Politecnica de Valencia–Campus de Gandia, Spain

(Received 22 September 2010; revised 28 July 2011; accepted 29 July 2011)

The phase angle component of the complex frequency response of a sonar system operating near transducer resonance is usually distorted. Interpretation and classification of the received sonar signal benefits from the preservation of waveform fidelity over the full bandwidth. A calibration process that measures the phase response in addition to the amplitude response is thus required. This paper describes an extension to the standard-target calibration method to include phase angle, without affecting the experimental apparatus, by using dual-frequency transmission pulses and frequency-domain data processing. This approach reduces the impact of unknown range and sound speed parameters upon phase calibration accuracy, as target phase is determined from the relationship of the two frequency components instead of relying on a local phase reference. Tungsten carbide spheres of various sizes were used to simultaneously calibrate the amplitude and phase response of an active sonar system in a laboratory tank. Experimental measurements of target phase spectra are in good agreement with values predicted from a theoretical model based upon full-wave analysis, over an operating frequency of 50–125 kHz. © *2011 Acoustical Society of America.*
[DOI: 10.1121/1.3628325]

PACS number(s): 43.30.Xm, 43.58.Vb, 43.30.Yj, 43.58.Ry [KGF] Pages: 1880–1887

I. INTRODUCTION

In conventional active sonar systems the phase angle of the echo reflected from the target is usually ignored. However, this approach would appear inconsistent with technological trends that aim to increase the information obtained from the environment, in order to facilitate human or algorithmic decision making. A complete analysis of the cues contained in an acoustic signal requires that both amplitude and phase are taken into account. The notion of augmented information is particularly relevant to the development of automatic acoustic means of fish or zooplankton species identification,[1] where target phase has been explored as a possible classifier.[2–5]

Before the physical significance of target phase can be successfully interpreted, it is imperative to address the effects of the entire sonar system including both the transducer and the electronic components. A calibration process that accounts for phase is required in order to ensure accurate and valid measurements.[4–6] Mathematically, the dynamics of a linear electro-acoustic system can be described in the frequency domain through its frequency or system response,[7,8] a complex variable composed of an amplitude and a phase, such as

$$H(f) = A(f)e^{j\Phi(f)}, \quad (1)$$

where $A(f)$ is the amplitude response and $\Phi(f)$ is the phase response. Existing procedures that estimate the complex sensitivity of hydrophones normally have to be implemented in specialized facilities, due to the technical challenges involved in the precise determination of phase.[9] In fisheries research and acoustical oceanography, the standard-target sonar calibration method[10] is well-established, but it does not address phase, examining only the scattering amplitude of the reference target. The inclusion of phase response to the standard-target method is also applicable to the calibration of multibeam sonar systems, in order to estimate the individual phase responses of array elements. This information is essential for the maintenance of sidelobe rejection performance within a beamformer,[9,11] which can undermine the directionality of a multibeam sonar and impact its quantitative capabilities.[12]

In more general terms, the calibration of phase is relevant to acoustic applications where the integrity of the temporal wave is important, such as in verifying the performance of specific waveforms, or in maintaining processing gain within a matched filter. It is also essential to ensure the exactitude of the phase response in studies,[13–15] where the information contained in the phase spectrum is exploited. The use of phase information has also been investigated in nondestructive testing, where additional cues contained in the phase can assist in the characterization of structural flaws.[16]

A. Phase distortions

A distortionless acoustic measurement system possesses a phase response, which is linearly related to frequency.[7]

[a]Author to whom correspondence should be addressed. Electronic mail: P.R.Atkins@bham.ac.uk

 0001-4966/2011/130(4)/1880/8/$30.00

The derivative of such a phase response with respect to frequency, called group or envelope delay, is a fixed value in time units proportional to the propagation interval of the signal through the system.[17] Deviations from a constant group delay, which occur in dispersive networks,[8] or media,[18] amount to phase distortions that imply fidelity degradation. That is, when the frequency components of a signal are delayed by disparate amounts of time the original shape of the waveform is modified, a phenomenon commonly encountered in systems with resonant transducer elements.[19]

In order to ameliorate waveform distortion, equalization techniques have been developed to correct the effects of the electronic circuitry, particularly when coupled to narrow-band transducers operating near resonance. For example, filter-derived matching networks have been investigated as a way to enhance phase response flatness while providing power matching.[20] Such networks are based on the classical electrical lumped-element transducer model,[21] with values that can be determined through impedance measurements. The connection of passive components to the transducer terminals, forming a band-pass filter, can contribute desirable characteristics to the overall response. Bessel filters, which exhibit a maximally flat group delay, would appear to be the optimal design approach.[20] In conjunction with passive matching networks, hardware and software equalization methods that compensate for the known effects of the system by predistorting the emitted signals have also been advanced.[22,23]

However, the corrective measures discussed previously may not be particularly convenient for application in commercial scientific echo sounders, as they rely on additional hardware, software compensation, and special transmission signals that may be less energy efficient, leading to a reduced noise-limited range performance. A more general treatment of phase distortion, instead of a case-by-case approach would be advantageous to sonar users and designers.

B. Phase calibration methods

The role of waveform distortion and phase spectra becomes more relevant with increased bandwidth utilization. For example, diagnostic medical ultrasound calibration techniques, based on time delay spectrometry and membrane hydrophone references, are applied in order to meet exacting phase flatness criteria.[24] As the desirability of phase calibration is appreciated to a greater extent, these methods have been implemented by internationally recognized metrological institutes, such as the Physikalisch-Technische Bundesanstalt in Germany,[25] whereas other techniques that previously were amplitude-only have also been adapted for the treatment of phase.[26] In general, the concept of full complex deconvolution has been advocated as the ideal approach.[27]

For the case of sonar hydrophones, the long-established calibration method of free-field reciprocity has also been extended to incorporate phase,[28] which constitutes the basis of the procedure used by the National Physical Laboratory, in the United Kingdom.[9] However, this technique is extremely sensitive to positioning accuracy and thus demands a typical alignment accuracy of better than one-hundredth of a wavelength.[11] An optical method developed in China, HAARI,[29] has similar performance but lower uncertainty levels, as the hydrophone is not required to rotate.[9] Nevertheless, the technique relies on a laser Doppler vibrometer, complicating its implementation outside a laboratory environment.

The standard-target calibration method is also fundamentally based on a deconvolution operation. The response of a reference target is obtained from a theoretical model based upon full-wave analysis solutions,[30,31] initially developed by Faran[32] and Hickling,[33] and reinstated correctly by Goodman and Stern.[34] The acoustic form function[35] (the normalized, steady-state, backscattered pressure as a function of frequency) is deconvolved from the measured signal either in the time domain[36] or with a complex division in the frequency domain.[31]

The standard-target method permits the determination of the complete system response, without incurring any additional uncertainties associated with the use of a reference hydrophone. This standard-target procedure is routinely implemented *in situ* before sonar surveys, with spherical reference targets usually made from electrolytic-grade copper, aluminum alloys, or tungsten carbide with 6% cobalt binder. It has been successfully adapted to modern broadband, multibeam sonar systems,[37,38] but in its current implementation it does not consider phase.

II. THEORY OF PHASE CALIBRATION WITH DUAL-FREQUENCY TRANSMISSIONS

Target phase can be calculated from the relative backscattered phases of a transmission pulse p_t composed of two frequencies, a lower f_1 and a higher $f_2 = \mu f_1$, expressed in the time domain as

$$p_t = \frac{V}{2}\cos(2\pi f_1 t) + \frac{V}{2}\cos(2\pi \mu f_1 t), \tag{2}$$

where t is time and V is the maximum amplitude of the voltage applied to the transducer. The spectral separation factor μ is usually defined as an integer ratio such as

$$\mu = \frac{N}{M}, \tag{3}$$

where N and M are small, typically within the range of 1–10.

Multifrequency transmission pulses for a phase-based estimation of range, or time delay, have been previously implemented in radar[39] and sonar[40] for localization and tracking purposes. Transmission signals with multiple harmonics are also employed in equivalent tasks by foraging bats such as the big brown bat.[41] In the context of underwater target identification these pulses were originally used to detect phase shifts induced by acoustically soft boundaries.[2,3] In these early works, dual-frequency transmissions were introduced because the time-axis asymmetry of such a pulse, shown in Fig. 1, allowed for easier detection of polarity reversals in the time domain. More recently, Atkins *et al.* refined the application of target phase as a classifier for underwater target identification.[5] They highlighted the fact that measuring the phase between the two frequency components of the transmitted signal removes range dependencies,

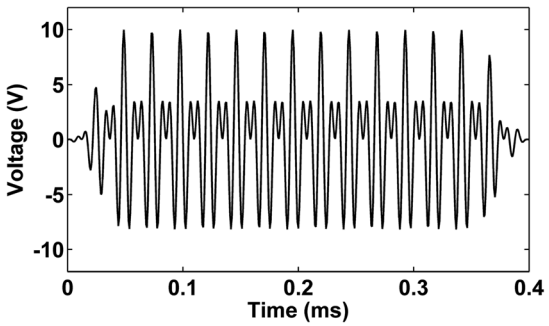

FIG. 1. Dual-frequency pulse, p_t, with frequency components $f_1 = 82$ kHz and $f_2 = 123$ kHz.

the source of many ambiguities in phase measurements, while dismissing the need of a local phase reference. These characteristics render this type of transmission signals suitable for phase calibration, suggesting their practicality in the extension of the standard-target method to include phase simultaneously with amplitude and without changing basic experimental settings. The elimination of the trend due to the phase accumulated during the progression of the signal, propagation phase,[42] leaves only the phase characteristics related to target and system effects.

Range dependencies are canceled following the method of Atkins *et al.*[5] After the received echo is windowed in time, subband correlators isolate the two frequency components to be compared, p_{r1} corresponding to the lower frequency and p_{r2} to the higher frequency. This pair of complex-valued components can be expressed as

$$p_{r1} = P_{r1} e^{j(k_1 r + \varphi_1)}, \tag{4}$$

$$p_{r2} = P_{r2} e^{j(k_2 r + \varphi_2)}, \tag{5}$$

where φ_1 *and* φ_2 are the target phases at each frequency, r is the range from the transmitter to the target, P_{r1} and P_{r2} are the peak received pressures, and k_1 and k_2 are the wave numbers in the water. In practice, this results in two receiver channels centered on frequencies separated by the factor μ, as exemplified in Fig. 2 for the case of the pulse presented in Fig. 1 ($f_1 = 82$ kHz and $f_2 = 123$ kHz). The bandwidth of the signals will be determined by the amplitude weighting function applied to the transmission signal, while the amplitudes will

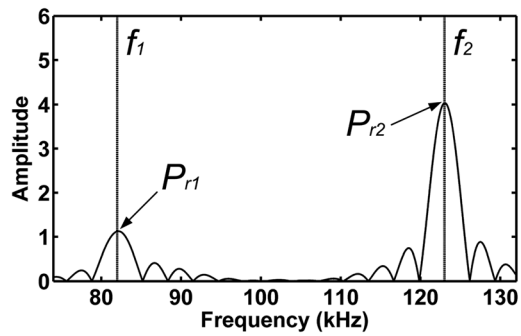

FIG. 2. Spectral magnitude components of a received echo from a 30-mm-diameter tungsten carbide sphere insonified by a dual-frequency pulse composed by $f_1 = 82$ kHz and $f_2 = 123$ kHz (spectral separation $\mu = 3/2 = 1.5$).

be influenced by the variations of the form function as the desired calibration bandwidth is covered with a series of stepped-frequency transmission pulses. In parallel to the processing of the measured data, the predicted phase response is calculated using the Goodman and Stern[34] model.

The next step in the determination of target phase is to scale the lower frequency component by μ and multiply it by the complex conjugate of the higher frequency component, such as

$$p_{r1\text{scaled}}\, p_{r2}^{*} = P_{r1}^{\mu} P_{r2} e^{j\mu(k_1 r + \varphi_1)} e^{-j(k_2 r + \varphi_2)}, \tag{6}$$

$$p_{r1\text{scaled}}\, p_{r2}^{*} = P_{r1}^{\mu} P_{r2} e^{j(\mu\varphi_1 - \varphi_2)}. \tag{7}$$

With this mathematical manipulation the range factor r is removed and a phase difference term, scaled by μ and corresponding solely to the target remains, such that

$$\text{angle}\left(p_{r1\text{scaled}}\, p_{r2}^{*}\right) = \mu\varphi_1 - \varphi_2 = \frac{N\varphi_1 - M\varphi_2}{M}, \tag{8}$$

where the "angle" operator yields a phase angle within the range from $-\pi$ to π.

In general terms, the scaled differential phase terms calculated and measured in this work are then defined as

$$\Delta\varphi_{\text{meas}}(f) = \frac{N\varphi_{\text{meas}}(f) - M\varphi_{\text{meas}}(\mu f)}{M} \tag{9}$$

and

$$\Delta\varphi_{\text{model}}(f) = \frac{N\varphi_{\text{model}}(f) - M\varphi_{\text{model}}(\mu f)}{M}, \tag{10}$$

where the subscripts "meas" and "model" refer to measured and modeled quantities, respectively. The resulting phase differences were used rather than absolute phases. These phases can be subsequently incorporated as a calibration data set into an experimental active sonar system simultaneously transmitting two frequency modulated waveforms with the same spectral separation value μ.

For amplitude calibration, one or both received frequency components can be used, as superposition applies and a condition of zero co-channel interference has been established. The system frequency response $H(f)$, which in this case includes the transducer and supporting electronics, as well as transmission losses, is extracted by a division in the frequency domain such as

$$H(f) = \frac{p_r(f)}{p_t(f) F_{\text{bs}}(f)}, \tag{11}$$

where all the variables are complex and a function of frequency f, p_r is the received pressure, p_t is the transmitted pressure, and F_{bs} is the backscattered form function in the far field. Although the function $H(f)$ is correspondingly complex and contains phase information, it remains ambiguous in range.

If we consider the pressure amplitude ratio of the measured received and transmitted pressures as the experimental

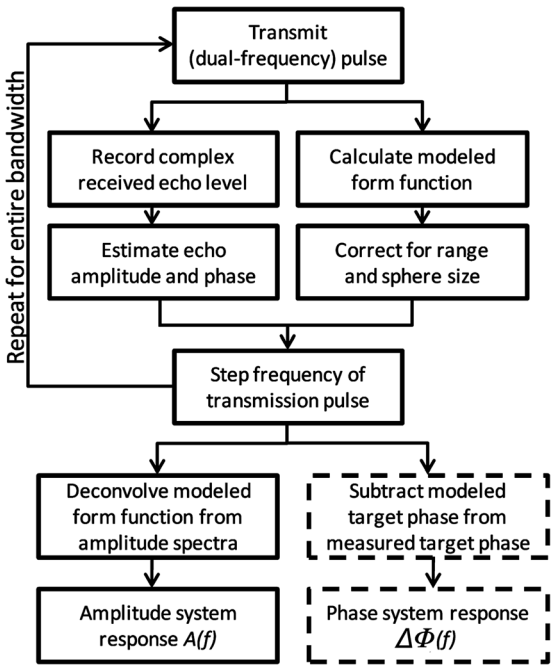

FIG. 3. Block diagram of the processing applied to the first set of backscattering measurements, in order to obtain the system amplitude and phase response. Subsequent measurements on other spheres followed the same steps, but the known effects of the system can now be removed in order to extract the calibrated target response. Dashed line boxes are for phase calibration only.

value to be recorded, the generality of the deconvolution method can be better illustrated as

$$p_{\text{ratio}}(f) = F_{\text{bs}}(f)H(f), \tag{12}$$

in which the expected value of the form function $F_{\text{bs}}(f)$ is affected by the response of the system, yielding the actual measured value, $p_{\text{ratio}}(f)$. For the case of phase the same relationship applies, but the measured and modeled phases are determined using dual-frequency transmission pulses. Thus, the expression that corresponds to Eq. (12) is

$$\Delta\varphi_{\text{meas}}(f) = \Delta\varphi_{\text{mod}}(f) + \Delta\Phi(f), \tag{13}$$

as phase angles can be added or subtracted instead of multiplied or divided, where $\Delta\Phi(f)$ is a function of the range-corrected value of the system phase response angle$[H(f)]$.[26] The system phase response can then be removed from subsequent measurements such that

$$\Delta\varphi_{\text{cal}}(f) = \Delta\varphi_{\text{meas}}(f) - \Delta\Phi(f), \tag{14}$$

in order to achieve a calibrated response, $\Delta\varphi_{\text{cal}}$, that can be compared with a predicted target phase. A simplified block diagram summarizing the procedures followed in this work and described in the previous paragraphs is shown in Fig. 3, with the steps added for phase calibration enclosed in parentheses and dashed lines.

III. EXPERIMENTAL METHOD

The experimental procedure follows the accepted practice of supporting a standard-target within the main lobe of the transducer.[10] The modifications introduced to obtain the system and target phase responses are the transmission of dual-frequency signals and the associated data processing. All experiments were conducted in the water tank at the University of Birmingham, with dimensions of 8.48 m in length, 3.95 m in width, and 3.04 m in depth. Targets were suspended with braided fishing lines made from high-modulus polyethylene fibers (Pure Fishing, Spirit Lake, IA) in order to prevent elongation, and attached to an XY table for alignment within the main lobe of a TC-2130 transducer (Reson, Slangerup, Denmark) with a central frequency of 100 kHz. The transducer acted both as transmitter and receiver and was encased in a frame padded with polyurethane acoustic absorber tiles (Applied Polymer Technology Limited, Ross On Wye, UK), in order to minimize the effects of boundary reverberation. The 30-mm-thick tiles were attached to the walls of the isolating cage around the transducer, as pictured in Fig. 4(B), providing reverberation reduction of approximately 40 dB within the measurement range window.

Pulses were generated and captured through a MATLAB (The Mathworks, Natick, MA) script, interfaced to a NI 6251 M-series data acquisition card (National Instruments, Austin, TX) with differential analog inputs and 16-bit analog outputs, both operating at 1.25 MHz sampling rate. Amplifiers, low-pass filters and a RX/TX switch control were custom-built for this experiment, with the main aim of enhancing noise performance. The differential amplifier in the return path (low-level signal) was battery-powered in order to avoid power-line noise. Temperature was monitored with a platinum resistor sensor connected to a Tracker 220 (TMS Europe, Bradwell, UK) that specifies an uncertainty of $\pm 0.075\,^{\circ}\text{C}$. The temperature was recorded at every frequency step and stored together with its associated

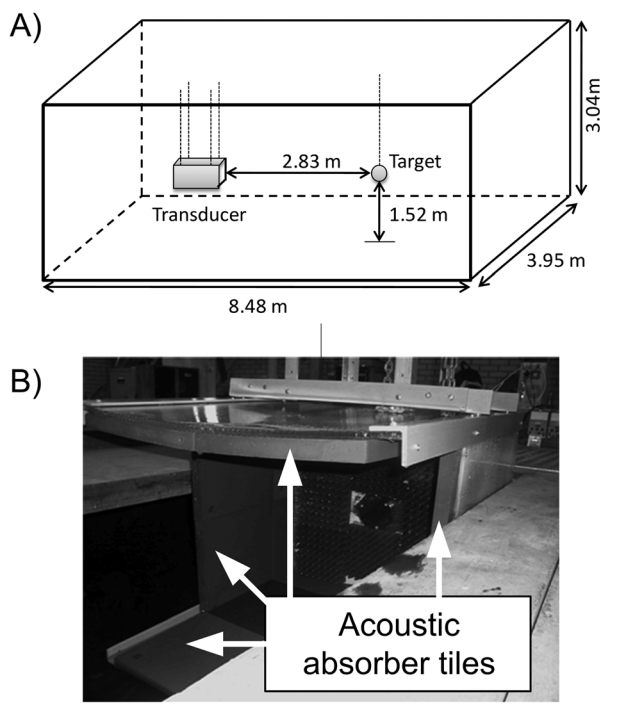

FIG. 4. (A) Schematic location of transducer and targets. (B) Transducer encased in antireverberation cage.

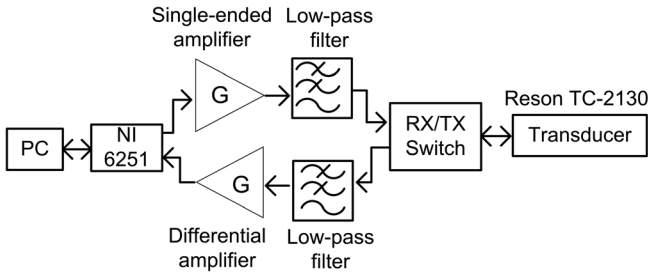

FIG. 5. Schematic of the complete electrical system. Signal generation and data acquisition operations are both performed through the NI 6251 data acquisition card. The sonar signal flow was controlled with the RX/TX switch, with logic signals also sent from the NI 6251. Amplifiers and filters were optimized for low-noise performance.

backscattering data. The temperature values were used in the calculation of the sound speed in the water, which is in turn an input to the Goodman and Stern computer model. This ensured that the modeled form function corresponded to the real experimental conditions, and that comparison with the recorded data did not introduce errors. The experimental and hardware configurations are depicted in Figs. 4 and 5, respectively.

As illustrated by the block diagram in Fig. 3, the system frequency response was obtained from an initial set of backscattering measurements performed on a 20-mm-diameter tungsten carbide sphere with 6% cobalt binder (Spheric Trafalgar, West Sussex, UK), this target being convenient because of its lack of resonances in the calibration bandwidth, 50–125 kHz ($\mu = 1.2$). The pulse duration was $T = 0.4$ ms, and the stepped-frequency increment was 500 Hz, with 10 pings being averaged for noise-reduction purposes. The amplitude and phase system responses, shown in Fig. 6, were first extracted and then applied to subsequent measurements (22-, 25-, 30-, and 40-mm-diameter tungsten carbide spheres with 6% cobalt binder from the same manufacturer), with results compared to the predicted response obtained from the theoretical model. The target remained stationary during insonification. Moving targets or platforms require more sophisticated processing strategies[5] that go beyond the scope of this paper.

IV. RESULTS AND DISCUSSION

For the determination of the responses presented in Fig. 6, a black box approach was adopted, in which a system transfer function represents all the stages contained in the two-way signal path. Therefore, all the hardware involved in the transmission and detection of the electroacoustical signal are included, as well as the purely acoustical effects of the water tank. Nevertheless, the magnitude characteristics [Fig. 6 (top panel)] show that the dominant factor is the transducer, as proven by the close resemblance to the manufacturer's data. For the case of phase, no equivalent specifications were available. The measured unwrapped differential phase response for the complete system [Fig. 6 (lower panel)] presents rapid changes of phase versus frequency, particularly around system poles and even where the magnitude curve is substantially flat. The approximate correspondence of peaks in the phase plot to points of inflection in the amplitude indicate minimum phase characteristics,[8] in combination with additional all-pass components.[19] These departures from a linear phase response, likely to appear in most practical systems due to the presence of various modes and interelement coupling,[6] further demonstrate the need for compensation.

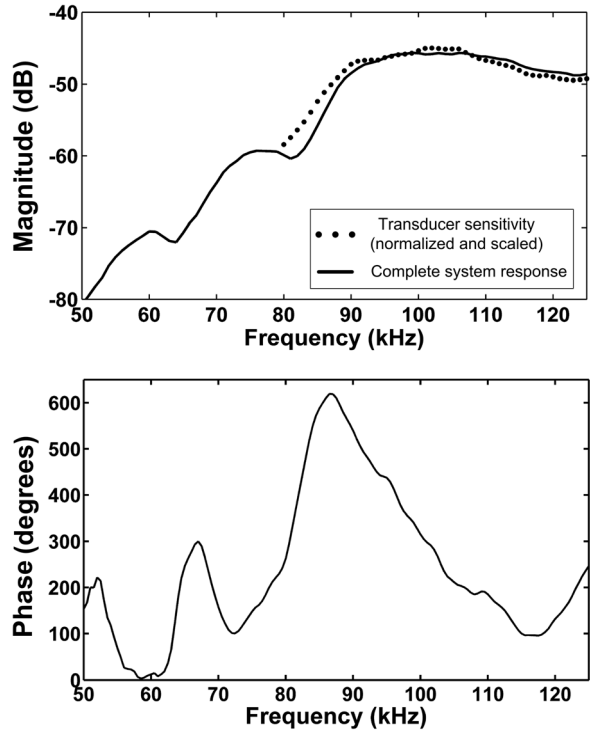

FIG. 6. (Top panel) Measured amplitude response of complete system, $20 \log[A(f)]$, including transducer, supporting electronics, and propagation losses in the tank (solid line), and transducer sensitivity from manufacturer's datasheet (dotted line). (Lower panel) Measured dual-frequency phase response of the system, $\Delta\Phi(f)$.

After the calibration procedure was performed, the error was estimated from the difference between the measured and modeled responses, using rms values. In amplitude, the rms target strength calibration error across the whole bandwidth was ~0.18 dB, when resonances were absent (22-mm-diameter sphere), and ~0.25 dB when resonances were present (25-mm-diameter sphere), values that are comparable to the potential, narrowband, accuracy of 0.1 dB.[43] These results support the notion that the target elastic resonances pose the most serious challenge for standard-target calibration accuracy in broadband sonar systems, due to the rapid variations in backscattered signal characteristics as a function of frequency. In order to minimize their detrimental effects the idea of separating the specular and resonant parts in the echo has been developed,[31] as well as the use of the joint response of multiple spheres.[44] In both approaches sensitivity to resonances is reduced. Other factors that can degrade the precision of amplitude calibration for broad band active sonar systems are mainly related to the level of knowledge and control of experimental conditions, as well as of the physical composition of the target.[43,45,46] As material parameters of the tungsten carbide spheres differ from the nominal values, the density of each sphere was measured and the transverse and longitudinal wave speeds in the solid were optimized via a multivariate minimization routine.

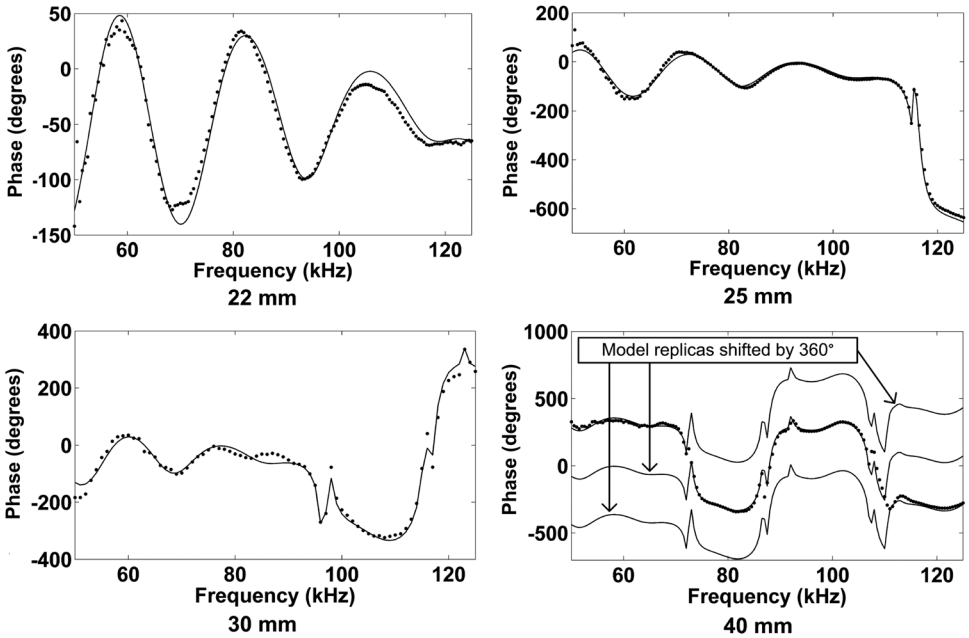

FIG. 7. Resulting agreement after calibration between the modeled and experimental phase responses, $\Delta\varphi_{\mathrm{mod}}(f)$ and $\Delta\varphi_{\mathrm{cal}}(f)$. Diameter of the spheres is indicated below each panel. Point plots correspond to calibrated measured data, solid lines to the Goodman and Stern model. For the case of the 40-mm-diameter sphere, modeled responses have been replicated and shifted by 360° in order to evince fit.

The agreement between measured and modeled phase difference values for other sizes of spheres is also reasonable, as shown in Fig. 7. It is clear that the agreement also tends to deteriorate as more resonances are included. For example, the rms error across the bandwidth is 9.58° for the 22-mm-diameter sphere, whereas it is 14.48° for the 25-mm-diameter sphere and 18.29° for the 30-mm-diameter sphere. Therefore, due to phase sensitivity to target composition, errors in the determination of these values can lead to calibration inaccuracies. It can be noticed in all plots that the lower-frequency section of the spectra is more conspicuously affected by noise, as the transducer sensitivity degrades as a function of frequency. Effects related to phase unwrapping are seen as 360° shifts. In the case of the 40-mm-diameter sphere, the measured data follow replicas of the modeled response scaled by 360°. Abrupt peaks in the curves are caused by the excitation of elastic resonances of the spheres,[47] as seen in all cases except for the 22-mm-diameter sphere.

It will be noted that a major advantage of the dual transmission frequency, standard-target method is that phase calibration errors do not increase as a function of frequency, only as a function of decreased signal-to-noise ratio and sphere resonances. This is further evidenced with the measured phase standard deviation, $s_{\mathrm{meas}}(f)$, presented in Fig. 8. As in the case of amplitude response, the interping variation of phase response also follows the system signal-to-noise ratio.

As mentioned previously, some of the issues affecting the accuracy and repeatability of amplitude calibration can also degrade the phase calibration. Nevertheless, the exactitude of phase calibration is also challenged by particular problems. For example, the presence of bubbles on the surface of the spheres can be an extraneous source of potential errors, as gas enclosures introduce acoustically soft characteristics to acoustically hard targets. In this respect, the practice of wetting and soaking the targets largely precludes the formation of bubbles and reduces stabilization time. Additional errors in phase determination can occur in reverberant environments where multipaths may contaminate the measured phase.[39] Moreover, operations such as frequency multiplication, performed on the processing of the dual subbands, can potentially magnify the effects of phase noise,[48] caused by fluctuations in oscillators and synthesizers, as well as external independent noise sources. In selecting the frequency separation values, the approach of maintaining spectrally independent subbands has been adopted, in order to avoid the correlation of noise. This approach is also advantageous in that it denies spectral overlapping (aliasing) issues. The processing strategy may also be viewed as that of multiplying both subband spectral components by factors such that a common phase comparison frequency is employed. Overall system phase-noise performance is improved when a lower phase comparison frequency is used, corresponding to a large value of μ, as the available bandwidth permits. This behavior is illustrated in Fig. 9, again in terms of phase standard deviation, where curves fitted to data sets from the same sphere (22 mm), but with different μ values, are shown. As expected, dual-frequency phase measurements obtained with a spectral factor of 1.5 present overall lower instability than those with 1.33 and 1.2. The system's intrinsic and

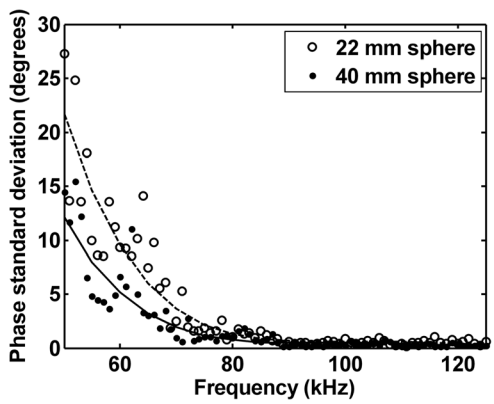

FIG. 8. Interping standard deviation of measured target phase, $s_{\mathrm{meas}}(f)$. Experimental data from 22 and 40 mm spheres with $\mu = 6/5 = 1.2$ shown together with their polynomial curve fits.

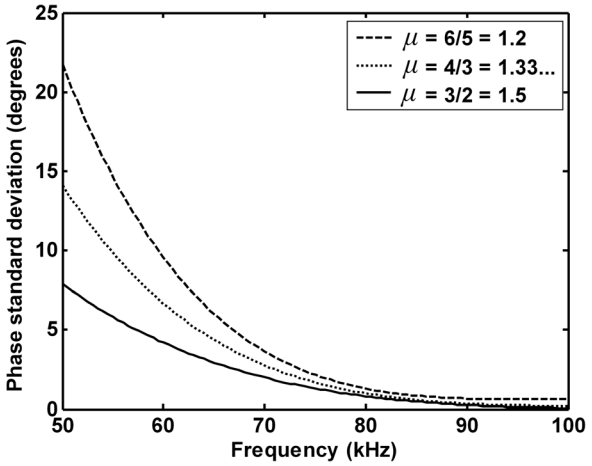

FIG. 9. Curve fits to measured phase standard deviation, $s_{\text{meas}}(f)$, from the 22 mm sphere at three different spectral separation values.

measured phase deviations, $s_{\text{int}}(f)$ and $s_{\text{meas}}(f)$ respectively, are related through the spectral separation such that

$$s_{\text{int}}(f) = \frac{s_{\text{meas}}(f)}{N+M}. \tag{15}$$

V. CONCLUSIONS

A phase calibration scheme has been proposed by conducting a standard-target calibration with frequency-stepped, pulsed continuous wave, dual-frequency transmissions. Target phase was determined from the subbands corresponding to each frequency component, removing range dependencies from measurements, and allowing for comparison with the phase spectra obtained from a theoretical model, also conducted in dual-frequency bands. Amplitude and phase calibration of a generic single-element active sonar system operating in a laboratory water tank was achieved, using tungsten carbide with 6% cobalt binder spheres as reference targets. Agreement between calibrated and predicted phase response is substantial, and although it is not anticipated that results obtained *in situ* (e.g., a sonar system installed in a vessel) would differ drastically, such tests remain pending for future work. The encouraging evidence from the present study highlights the flexibility of the standard-target method, as adapted to the calibration of phase, with a precision that is primarily constrained by the knowledge of the material parameters of the reference target, sensitivity to mechanical resonances, and signal-to-noise ratio. Other topics of interest would be the use of different reference targets, such as air-filled shells,[49] and the possibility of adapting this phase calibration method to the time domain, especially to systems relying on short broadband pulses.[31,35]

ACKNOWLEDGMENTS

The authors would like to thank Dr. Trevor Francis for his insight and valuable help with the computer script of the theoretical model. A.I.-C. gratefully acknowledges funding provided by the Mexican National Committee for Science and Technology (CONACYT).

[1]J. K. Horne, "Acoustic approaches to remote species identification: A review," Fish. Oceanogr. **9**, 356–371 (2000).
[2]D. G. Tucker and N. J. Barnickle, "Distinguishing automatically the echoes from acoustically 'hard' and 'soft' objects with particular reference to the detection of fish," J. Sound. Vib. **9**, 393–397 (1969).
[3]H. Braithwaite, "Discrimination between sonar echoes from fish and rocks on the basis of 'hard' and 'soft' characteristics," J. Sound Vib. **27**, 549–557 (1973).
[4]R. Barr and R. F. Coombs, "Target phase: An extra dimension for fish and plankton target identification," J. Acoust. Soc. Am. **118**, 1358–1371 (2005).
[5]P. R. Atkins, T. Collins, and K. G. Foote, "Transmit-signal design and processing strategies for sonar target phase measurement," IEEE J. Sel. Top. Signal Process. **1**, 91–104 (2007).
[6]P. R. Atkins, K. G. Foote, and T. Collins, "Practical implications of sonar target-phase measurement classifiers," in *Proceedings of the Institute of Acoustics International Conference on Detection and Classification of Underwater Targets*, Edinburgh, Scotland, 2007, Vol. 29, Part 6, pp. 163–172.
[7]A. Papoulis, *The Fourier Integral and its Applications* (McGraw-Hill, London, 1962, pp. 1–318.
[8]R. C. Heyser, "Loudspeaker phase characteristics and time delay distortion: Part 1," J. Audio Eng. Soc. **17**, 30–41 (1969).
[9]G. Hayman and S. P. Robinson, "Phase calibration of hydrophones by the free-field reciprocity method in the frequency range 10 kHz to 400 kHz," National Physical Laboratory Report No. AC 1 (2007).
[10]K. G. Foote, H. P. Knudsen, G. Vestnes, D. N. MacLennan, and E. J. Simmonds, "Calibration of acoustic instruments for fish density estimation: A practical guide," ICES Coop. Research Report No. 144 (1987).
[11]P. Pocwiardowski, G. Yufit, E. Maillard, and P. Eriksen, "Method for large sonar calibration and backscattering strength estimation," *Proceedings of the MTS/IEEE Oceans (2006) Conference*, pp. 1–5.
[12]N. A. Cochrane, Y. Li, and G. D. Melvin, "Quantification of a multibeam sonar for fisheries assessment applications," J. Acoust. Soc. Am. **114**, 745–758 (2003).
[13]N. Yen, L. R. Dragonette, and S. K. Numrich, "Time-frequency analysis of acoustic scattering from elastic objects," J. Acoust. Soc. Am. **87**, 2359–2370 (1990).
[14]G. Maze, "Acoustic scattering from submerged cylinders. MIIR Im/Re: Experimental and theoretical study," J. Acoust. Soc. Am. **89**, 2559–2566 (1991).
[15]F. G. Mitri, J. F. Greenleaf, Z. E. A. Fellah, and M. Fatemi, "Investigating the absolute phase information in acoustic wave resonance scattering," Ultrasonics **48**, 209–219 (2008).
[16]N. Mercier, J. F. de Belleval, and P. Lanceleur, "Characterization of flaws using the poles and zeros of the transfer function of the corresponding ultrasonic system," Ultrasonics **31**, 229–235 (1993).
[17]R. C. Heyser, "Loudspeaker phase characteristics and time delay distortion: Part 2," J. Audio Eng. Soc. **17**, 130–137 (1969).
[18]L. Brillouin, *Wave Propagation and Group Velocity* (Academic, London, 1960), pp. 1–16.
[19]J. Blauert and P. Laws, "Group delay distortions in electroacoustical systems," J. Acoust. Soc. Am. **63**, 1478–1483 (1978).
[20]P. R. Atkins, A. Islas-Cital, and K. G. Foote, "Sonar target-phase measurement and effects of transducer matching," J. Acoust. Soc. Am. **123**, 3949(A) (2008).
[21]D. Stansfield, *Underwater Electroacoustic Transducers* (Bath University Press, Bath, UK, 1991), pp. 73–141.
[22]P. E. Doust and J. F. Dix, "The impact of improved transducer matching and equalisation techniques on the accuracy and validity of underwater acoustic measurements," in *Proceedings of the Institute of Acoustics Conference on Acoustical Oceanography*, Southampton, UK, 2001, Vol. 23, Part 2, pp. 100–109.
[23]S. Assous, D. Gunn, C. Hopper, P. D. Jackson, L. Linnet, and M. Lovell, "An approach for correcting magnitude and phase distortion in wideband piezoelectric transducer systems," *Proc. OES/IEEE Oceans 2007 Conf.*, pp. 1543–1548 (2007).
[24]V. Wilkens and C. Koch, "Amplitude and phase calibration of hydrophones up to 70 MHz using broadband pulse excitation and an optical reference hydrophone," J. Acoust. Soc. Am. **115**, 2892–2903 (2004).
[25]Anon., "Short report for CCAUV—September 2008," Physikalisch-Technische Bundesanstalt, 2008, pp. 1–7.
[26]M. P. Cooling and V. F. Humphrey, "A nonlinear propagation model-based phase calibration technique for membrane hydrophones," IEEE Trans. Ultrason., Ferroelect., Freq. Contr. **55**, 84–93 (2008).
[27]A. Hurrell, "Voltage to pressure conversion: Are you getting 'phased' by the problem?" J. Phys.: Conf. Series, Adv. Metrol. Ultrasound Med. **1**, 57–62 (2004).

[28]L. D. Luker and A. L. Van Buren, "Phase calibration of hydrophones," J. Acoust. Soc. Am. **70**, 516–519 (1981).
[29]W. Yuebing and H. Yongjun, "The application of optical interferometry in the measurement of hydrophones," in *Proceedings of the Institute of Acoustics Conference on Calibration and Measurement in Underwater Acoustics*, London, UK, 2003, Vol. 25, Part 1, pp. 10–18.
[30]K. G. Foote, "Optimizing copper spheres for precision calibration of hydroacoustic equipment," J. Acoust. Soc. Am. **71**, 742–747 (1982).
[31]T. K. Stanton and D. Chu, "Calibration of broadband active acoustic systems using a single standard spherical target," J. Acoust. Soc. Am. **124**, 128–136 (2008).
[32]J. J. Faran, Jr., "Sound scattering by solid cylinders and spheres," J. Acoust. Soc. Am. **23**, 405–418 (1951).
[33]R. Hickling, "Analysis of echoes from a solid elastic sphere in water," J. Acoust. Soc. Am. **34**, 1582–1592 (1962).
[34]R. R. Goodman and R. Stern, "Reflection and transmission of sound by elastic spherical shells," J. Acoust. Soc. Am. **34**, 338–344 (1962).
[35]H. D. Dardy, J. A. Bucaro, L. S. Schuetz, and L. R. Dragonette, "Dynamic wide-bandwidth acoustic form-function determination," J. Acoust. Soc. Am. **62**, 1373–1376 (1977).
[36]C. Feuillade, R. W. Meredith, N. P. Chotiros, and C. S. Clay, "Time domain investigation of transceiver functions using a known reference target," J. Acoust. Soc. Am. **112**, 2702–2712 (2002).
[37]K. G. Foote, D. Chu, T. R. Hammar, K. C. Baldwin, L. A. Mayer, L. C. Hufnagle, Jr., and J. M. Jech, "Protocols for calibrating multibeam sonar," J. Acoust. Soc. Am. **117**, 2013–2027 (2005).
[38]E. Ona, V. Mazauric, and L. N. Andersen, "Calibration methods for two scientific multibeam systems," ICES J. Mar. Sci. **66**, 1326–1334 (2009).
[39]Y. Zhang, M. Amin, and F. Ahmad, "Time-frequency analysis for the localization of multiple moving targets using dual-frequency radars," IEEE Signal Proc. Lett. **15**, 777–780 (2008).
[40]S. Assous, C. Hopper, M. Lovell, D. Gunn, P. Jackson, and J. Rees, "Short pulse multi-frequency phase-based time delay estimation," J. Acoust. Soc. Am. **127**, 309–315 (2010).
[41]W. W. L. Au and J. A. Simmons, "Echolocation in dolphins and bats," Phys. Today **60**, 40–45 (2007).
[42]R. H. Lyon, "Progressive phase trends in multi-degree-of-freedom systems," J. Acoust. Soc. Am. **73**, 1223–1228 (1983).
[43]K. G. Foote, "Maintaining precision calibrations with optimal copper spheres," J. Acoust. Soc. Am. **73**, 1054–1063 (1983).
[44]P. R. Atkins, D. T. I. Francis, and K. G. Foote, "Calibration of broadband sonar systems using multiple standard targets," J. Acoust. Soc. Am. **123**, 3436(A) (2008).
[45]H. Hobæk and T. L. Nesse, "Scattering from spheres and cylinders—revisited," *Proceedings of the Norwegian Physics Society 29th Symposium on Physical Acoustics*, 2006, pp. 1–16.
[46]A. Islas-Cital, P. R. Atkins, and K. Y. Foo, "Standard target calibration of broad-band active sonar systems in a laboratory tank," *Proceedings of the OES/IEEE Oceans 2010 Conference*, 2010, pp. 1–10.
[47]L. Flax, L. R. Dragonette, and H. Uberall, "Theory of elastic resonance excitation by sound scattering," J. Acoust. Soc. Am. **63**, 723–731 (1978).
[48]A. L. Lance, W. D. Seal, and F. Labbar, "Phase noise and AM noise measurements in the frequency domain," Int. J. Infrared Millim. Waves **11**, 239–289 (1984).
[49]P. R. Atkins, D. T. I. Francis, and K. G. Foote, "Broadband ultrasonic target strengths of hollow ceramic flotation spheres," *Proceedings of the OES/IEEE Oceans 2007 Conference*, 2007, pp. 1–4.